

Optimum Design of the Involute-Cycloid Composite Tooth Profile Helical Gear

Florin G. TUTULAN*, Kazuteru NAGAMURA** and Kiyotaka IKEJO***

The tooth bending and tooth contact strengths of the involute-cycloid composite tooth profile helical gear, which was developed as a non-involute tooth profile gear based on cycloid tooth profile, are directly affected by its tooth profile. The involute-cycloid composite tooth profile curve changes with some design parameters such as pressure angle and radius of rolling circle. In this study, we developed a method to calculate the tooth root stress and the tooth contact stress of the involute-cycloid composite tooth profile helical gear. Then we compared the tooth root and tooth contact stresses calculated by this method with the experimentally measured data, and the validity of the present calculation method was certified by the good agreement of the calculated values with the measured data. Furthermore, we discussed the effects of the design parameters on the tooth bending and tooth contact strengths of the involute-cycloid composite tooth profile helical gear considering the results of the tooth root and the tooth contact stresses calculated in the case of various values of the design parameters.

Key words: Gear, Non-Involute Helical Gear, Involute-Cycloid Composite Tooth Profile, Bending Strength, Tooth Contact Strength

1. Introduction

Involute gears have been widely used because of their advantages, such as, ease of manufacture and the fact that the gear speed is unchanged even if the gear center distance changes, etc. However, involute gears have several disadvantages: the sliding on the teeth is greater, the surface durability is lower, and the undercut occurs more frequently in gears having a small number of teeth compared to other tooth profile gears. In a previous study¹⁾, we developed a non-involute helical gear that had an involute-cycloid composite tooth profile shown in Fig. 1.

In this study, we have improved the tooth profile design by changing design parameters such as pressure angle and rolling circle, which define the involute-cycloid composite tooth profile curve, to decrease the tooth root stress of the involute-cycloid composite tooth profile helical gear. Due to economical considerations, first we developed a computer program for designing the tooth profile. The tooth root stresses calculated by the computer program were compared with measured values and the validity of this calculation method was examined. After that, we investigated the effects of the design parameters on the tooth bending and tooth contact strengths of the

involute-cycloid composite tooth profile helical gear using the computer program.

2. Involute-Cycloid Composite Tooth Profile

The involute-cycloid composite tooth profile consists of an involute tooth profile near the pitch point and a cycloid tooth profile at the addendum and the dedendum, as shown in Fig. 1. Figure 2 shows the basic rack form for the involute-cycloid composite tooth profile gear. The rack for the composite tooth profile gear is of the form PQR' consisting of a straight line PQ and a cycloid curve QR' which is drawn by rolling a circle on the x -axis (the base pitch line).

The addendum and the dedendum of the rack are symmetric to each other with respect to the pitch point P because of the interchangeability of gear¹⁾.

Using the coordinate system shown in Fig. 2, the cycloid curve P'QR' is expressed as follows:

$$\left. \begin{aligned} x &= a(\theta - \sin \theta) + X_0 \\ y &= a(1 - \cos \theta) \end{aligned} \right\} \quad (1)$$

where a is the radius of the rolling circle; θ is the rotational angle of the rolling circle; and α_0 is the inclination of the straight line PQ to the y -axis, equal to the cutter pressure angle of involute.

* Doctor student, Mechanical System Engineering, Hiroshima University

** Professor, Mechanical System Engineering, Hiroshima University

*** Research Associate, Mechanical System Engineering, Hiroshima University

In addition, the straight line PR is expressed as follows:

$$y = x \cot \alpha_0 \quad (2)$$

X_0 shown in Fig. 2 and in the equation (1) is the distance between the pitch point P and the point P' where the cycloid curve begins, and Y_0 is the distance between the base pitch line (x-axis) and the point Q connecting the cycloid curve QR' and the straight line PQ. The distances X_0 and Y_0 can be derived from the equations (1) and (2) as follows:

$$\left. \begin{aligned} X_0 &= 2a \operatorname{inv} \alpha_0 \\ Y_0 &= a(1 - \cos 2\alpha_0) \end{aligned} \right\} \quad (3)$$

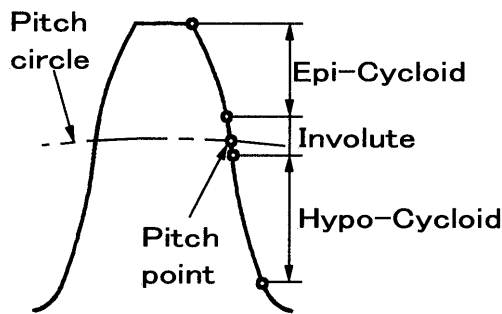


Fig. 1 Involute-cycloid composite tooth profile helical gear

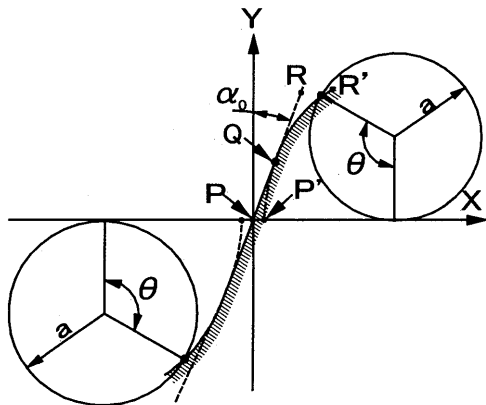


Fig. 2 Basic rack form of involute-cycloid composite tooth profile helical gear

3. Tooth Root Stress of the Involute-Cycloid Composite Tooth Profile Helical Gear

3.1 Calculation method of the tooth root stress

The tooth root stresses σ_t and σ_c on tensile and compressive sides of the involute-cycloid composite

tooth profile helical gear can be expressed with the following equation (4):

$$\left. \begin{aligned} \sigma_t &= \alpha_{tb} \frac{6M}{S_F^2} \\ \sigma_c &= \alpha_{cb} \frac{6M}{S_F^2} \end{aligned} \right\} \quad (4)$$

where α_{tb} and α_{cb} are the stress concentration factors, S_F is the tooth thickness on the critical section at the tooth fillet and M is the bending moment at the tooth fillet.

As for the stress concentration factors α_{tb} and α_{cb} , the following approximations are used²⁾:

$$\alpha_{tb} = \frac{\sigma_{to}}{\sigma_{tNb}}, \quad \alpha_{cb} = \frac{\sigma_{co}}{\sigma_{cNb}} \quad (5)$$

where σ_{tNb} and σ_{cNb} are the nominal bending tooth root stresses of virtual spur gear and σ_{to} and σ_{co} are the tooth root stresses of virtual spur gear^{3),4)}.

The bending moment M is calculated using the moment image method⁵⁾ as follows:

$$M = \gamma \cdot P \quad (6)$$

where P is the concentrated load and γ is named the influence function of bending moment at tooth fillet.

3.2 Calculation result of the tooth root stress

Table 1 shows the dimensions of the involute-cycloid composite tooth profile helical gears used in the calculation and the experiment.

Table 1 Specification of helical gears (in the transverse plane)

		Involute	Involute-cycloid composite
Module	m_t (mm)	4.042	4
Pressure angle	α_0 (deg)	22.8	13
Number of tooth	z_1/z_2	29/29	29/29
Radius of rolling circle	a (mm)	-	7
Helix angle	β (deg)	30	30
Addendum	h_a (mm)	0.670m	1.0m
Dedendum	h_f (mm)	1.264m	1.1m
Addendum modification coefficient		-0.18	-
Pitch circle diameter	d (mm)	117.2	116
Face width	b (mm)	20	20
Tip circle diameter	d_a (mm)	122.6	124
Total contact ratio	ϵ	2.255	2.129
Material & Heat treatment		S45C Thermal refining	S45C Thermal refining
Method of finishing teeth		Hobbing	Hobbing

* Value at pitch point

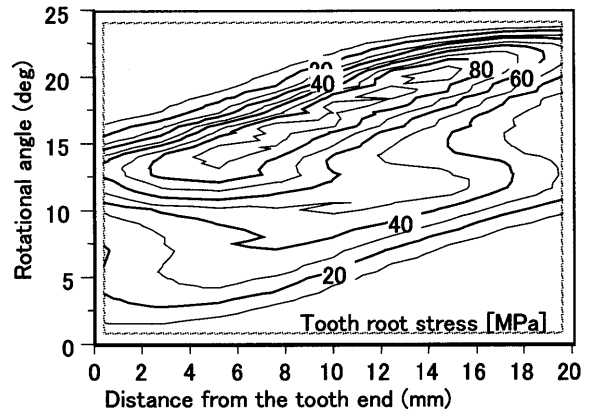
Figure 3 compares the tooth root stress calculated by the present method with the experimental results. As seen from this figure, the calculation results of the tooth root stress are in good agreement with the experimental results. Some minor disagreements between the calculation results and the experimental results in Fig. 3 may be due to the calculation without

considering gear error and alignment error. Therefore, the validity of the present calculation method is proved.

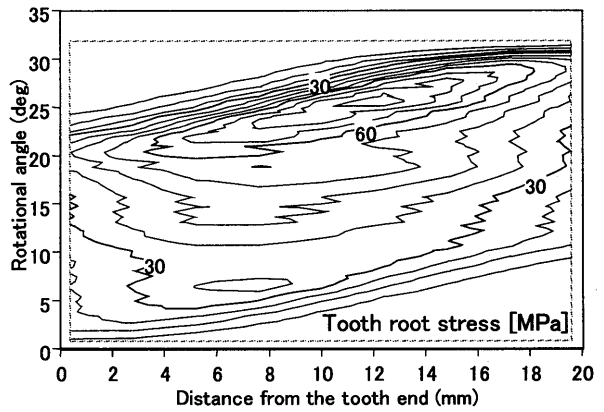
Figures 4 (a) and (b) show the calculated tooth root stress of the involute-cycloid composite tooth profile helical gear for different values of the radius of the rolling circle a . The abscissa denotes the distance from one tooth end to the other tooth end along the face width on the tooth fillet, and the ordinate represents the rotational angle of the driving gear.

In order to investigate the effect of pressure angle α_0 and radius of rolling circle a , the tooth root stresses were calculated for different values of these parameters. The calculated tooth root stresses for gears having various radii of rolling circle a , and different values of pressure angle α_0 is shown in Fig. 5. The maximum tooth root stress decreases with the increase of the values of pressure angle and radius of rolling circle, except for $\alpha_0 = 10^\circ$ where the tooth root stress remains almost constant.

Figure 6 represents three profiles of the involute-cycloid composite tooth profile helical gear having different values for the radius of the rolling circle but the same value for the pressure angle. Figure 7 also shows three profiles of the involute-cycloid composite tooth profile helical gear having different values of the pressure angle but the same value for the radius of the rolling circle.



(a) $m_t=4$ mm, $\alpha_0=13^\circ$, $a=5$ mm, $T=98$ Nm



(b) $m_t=4$ mm, $\alpha_0=13^\circ$, $a=16$ mm, $T=98$ Nm

Fig. 4 Calculation results of tooth root stress

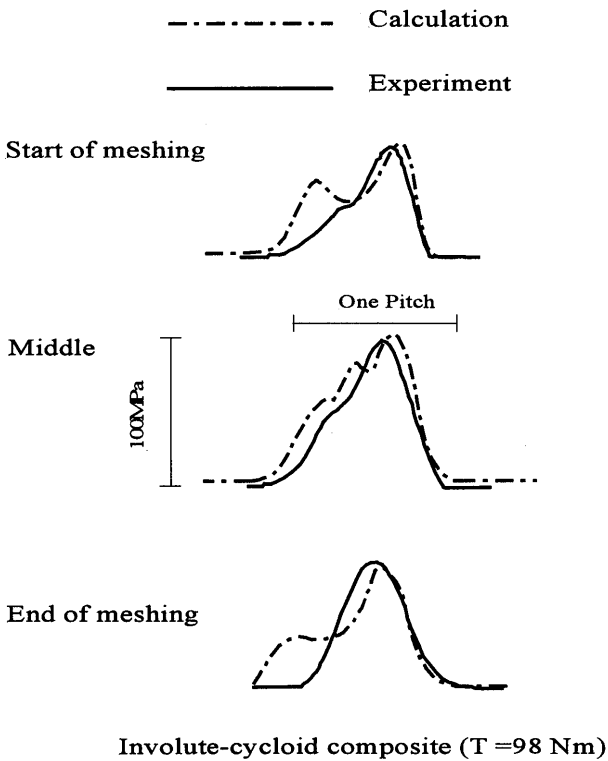


Fig. 3 Comparison of tooth root stress waveform between experimental and calculation results ($m_t=4$ mm, $\alpha_0=13^\circ$, $a=7$ mm)

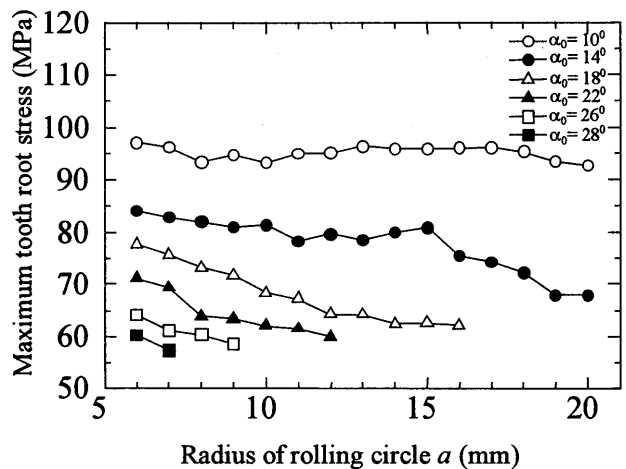


Fig. 5 Variation of tooth root stress ($T=98$ Nm)

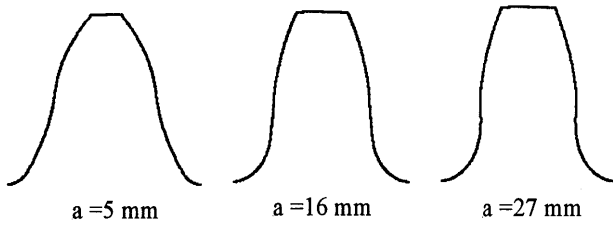


Fig. 6 Tooth profile of involute-cycloid composite helical gear ($z=29, \alpha_0=13^\circ$)

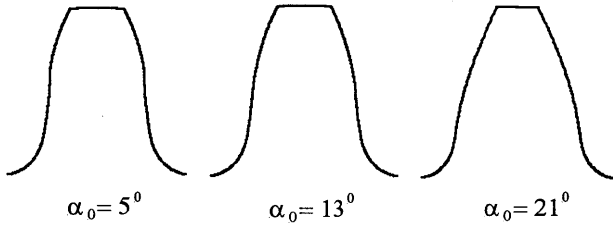


Fig. 7 Tooth profile of involute-cycloid composite helical gear ($z=29, a=13\text{mm}$)

4. Tooth Contact Stress of the Involute-Cycloid Composite Tooth Profile Helical Gear

4.1 Calculation method of tooth contact stress

The tooth contact stress can be obtained by following equation:

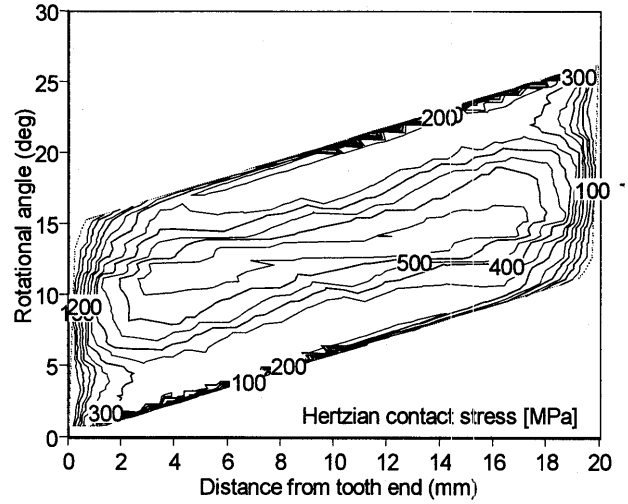
$$\sigma_H = \frac{1.273 \cdot p}{a_H} \quad (7)$$

where p is the distributed load on tooth and $a_H=2a_c$ is the Hertzian contact width³⁾.

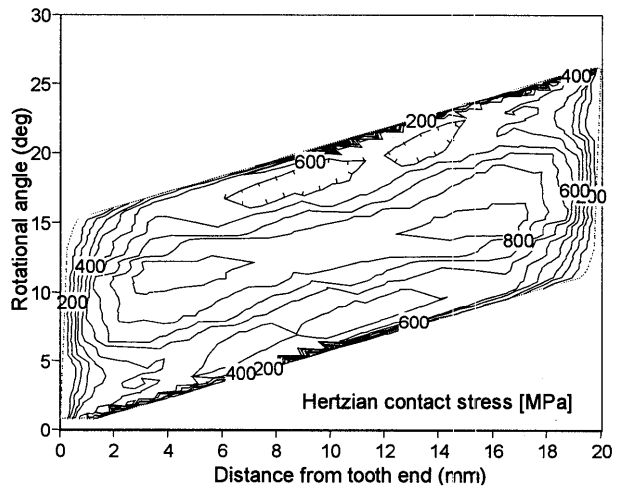
4.2 Calculation result of tooth contact stress

The calculated tooth contact stress of the involute-cycloid composite tooth profile helical gear is shown in Fig. 8. The abscissa denotes the distance from one tooth end to the other tooth end along the face width and the ordinate represents the rotational angle of the driving gear. As seen from Fig. 8, the tooth contact stress has the maximum value at a certain point along the face width and decreases at both tooth ends.

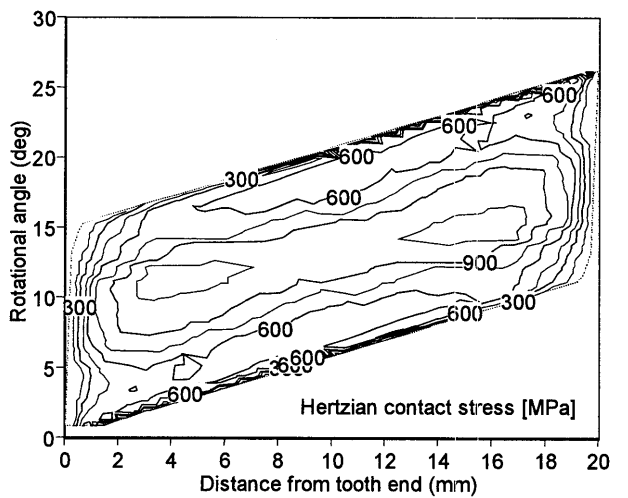
Figures 9 and 10 show the calculated tooth contact stresses for gears having various radii of rolling circle a and different values of pressure angle α_0 . From Fig. 9 the maximum tooth contact stress has a peak value for a radius of rolling circle $a=7$ mm and it decreases when the value of radius of rolling circle becomes larger than 7 mm. For $\alpha_0=14^\circ$ the maximum tooth contact stress has a peak value for a radius of rolling circle $a=7$ mm. From Fig. 10 the maximum tooth contact stress has a peak value for a radius of rolling circle $a=7$ mm and it decreases rapidly when the value of radius of rolling circle becomes larger than 7 mm.



(a) $T=294$ Nm



(b) $T=588$ Nm



(c) $T=735$ Nm

Fig. 8 Calculation result of tooth contact stress σ_H ($\alpha_0=13^\circ, a=7$ mm)

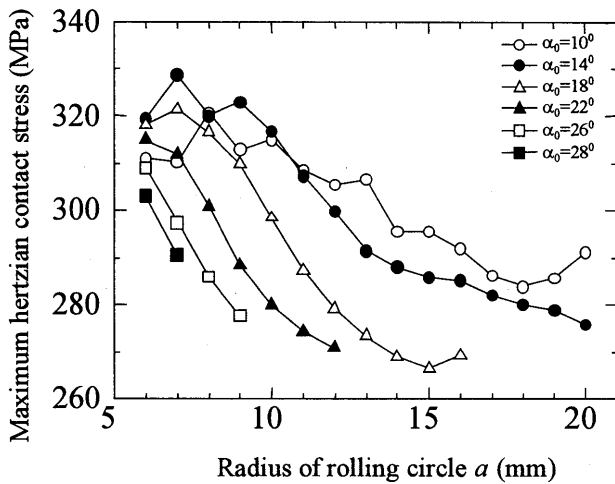


Fig. 9 Variation of tooth contact stress ($T=98\text{ Nm}$, $\alpha_0=10\sim 28^\circ$)

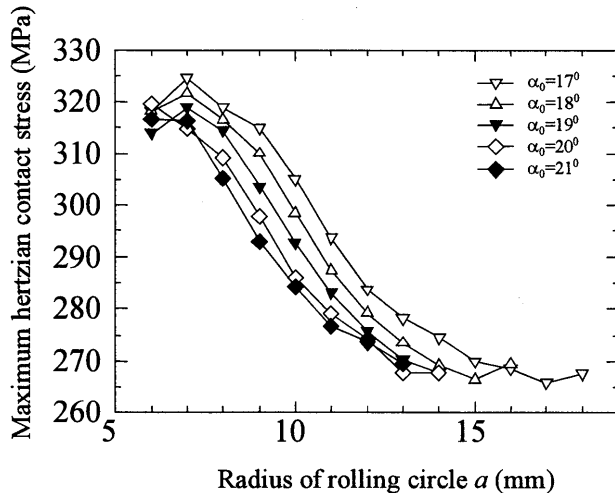


Fig. 10 Variation of tooth contact stress ($T=98\text{ Nm}$, $\alpha_0=17\sim 21^\circ$)

5. Comparison between the Results of the Involute Cycloid Composite Tooth Profile Helical Gear and the Involute Helical Gear

The tooth root stress waveform of the involute helical gear is shown in Fig. 11 by comparison between experimental and calculation results. Also for the involute helical gear, the calculation results of the tooth root stress are in good agreement with the experimental results. The tooth root stress waveform of the involute-cycloid composite tooth profile helical gear is shown in Fig. 12 for different values of the pressure angle α_0 and the radius of the rolling circle a .

Table 2 shows the calculated values of the tooth root stress and tooth contact stress for the involute helical gear and for the involute-cycloid composite

tooth profile helical gears with different values of pressure angle α_0 and radius of rolling circle a . The tooth root stress for the involute-cycloid composite helical gear is inferior to that of the involute helical gear but the tooth contact stress is superior to the involute helical gear. The tooth root stress decreases significantly for a higher value of the pressure angle. The tooth contact stress also decreases significantly for a higher value of the pressure angle and a larger value of the radius of rolling circle.

Table 2 Calculation results of tooth root stress and tooth contact stress ($T=98\text{ Nm}$)

	Involute	Involute cycloid composite		
		$\alpha_0=13^\circ$ $a=7\text{ mm}$	$\alpha_0=28^\circ$ $a=7\text{ mm}$	$\alpha_0=17^\circ$ $a=17\text{ mm}$
Tooth root stress (MPa)	49.66	85.37	57.40	63.09
Hertzian contact stress (MPa)	551.64	318.76	290.66	265.78

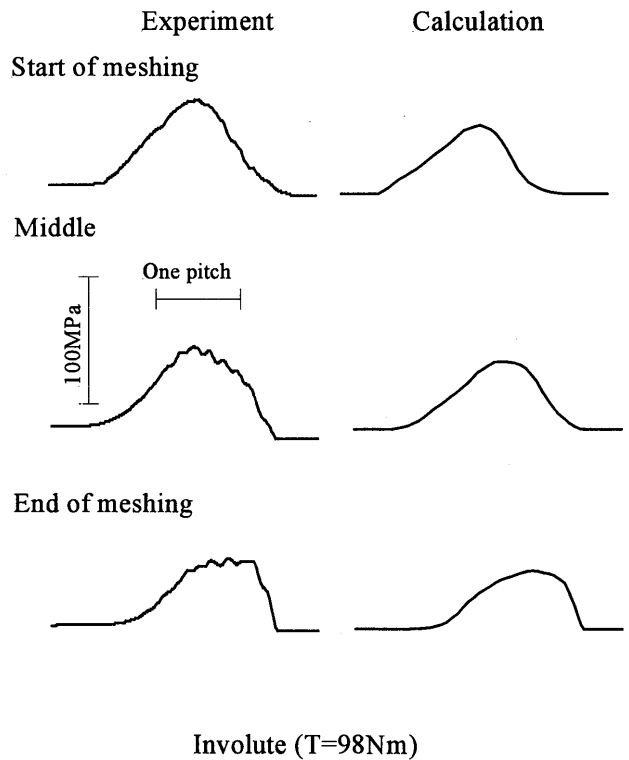


Fig. 11 Tooth root stress waveform of involute helical gear

6. Conclusions

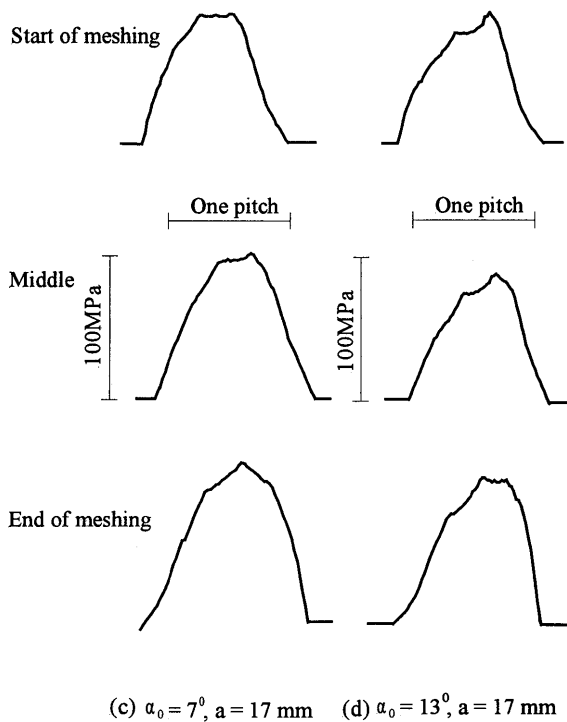
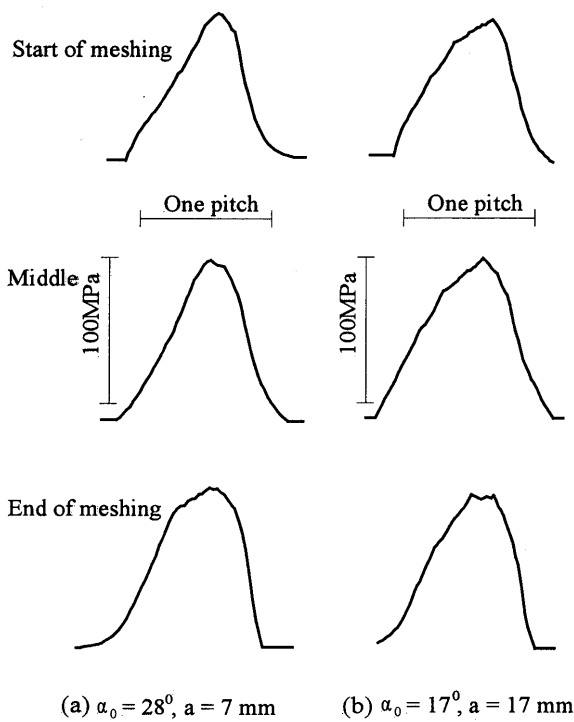
The main conclusions are:

(1) In this study, a general calculating method has been developed for predicting tooth root stress and tooth contact stress of the involute-cycloid composite tooth profile helical gear without considering manufacturing and alignment errors.

(2) Comparison between measured and calculated results showed good agreement for tooth root stress.

(3) It is confirmed in this study that the tooth contact stress of the involute-cycloid composite tooth profile helical gear is superior to the involute helical gear. However, although the tooth root stress of the involute-cycloid composite tooth profile helical gear is significantly improved by using appropriate values of design parameters, it is still inferior to the involute helical gear.

(4) The tooth root stress decreases significantly for a higher value of the pressure angle. The tooth contact stress decreases rapidly for a higher value of the pressure angle and a larger value of the radius of rolling circle.



Involute-cycloid composite ($T = 98 \text{ Nm}$)

Fig. 12 Tooth root stress waveform for different values of pressure angle α_0 and radius of rolling circle a

References

- 1) Tutulan, F. G, Nagamura, K., Ikejo, K., (2004), "Vibration Characteristics and Surface Durability of Non-Involute Helical Gears", (submitted for publication).
- 2) Kubo, A., (1978), "Stress Condition, Vibrational Exciting Force, and Contact Pattern of Helical Gears with Manufacturing and Alignment Error", ASME Journal of Mechanical Design, **100**, pp. 77-84.
- 3) Aida, T., Terauchi, Y., (1962), "On the Bending Stress of a Spur Gear", Bulletin of JSME, **5**, No. 17, pp. 161-183.
- 4) Aida, T., Oda, S., Tamura, Y., (1967), "Study on Bending Fatigue Strength of Gears (8th Report, Practical Formula for True Compressive Root Stress and Experiment)", Trans. JSME (in Japanese), **33**, No. 252, pp. 1321-1330.
- 5) Umezawa, K., (1973), "The Meshing Test on Helical Gears under Load Transmission (2nd Report, The Approximate Formula for Bending-Moment Distribution of Gear Tooth)", Bulletin of JSME, **16**, pp. 407-413.

Received Sept. 30, 2004